POSSIBLE EFFECTS OF IRON FERTILIZATION IN THE SOUTHERN OCEAN ON ATMOSPHERIC CO_2 CONCENTRATION

Fortunat Joos and Ulrich Siegenthaler

Physics Institute, University of Bern
Bern, Switzerland

Jorge L. Sarmiento

Atmospheric and Ocean Sciences Program
Princeton University, Princeton, New Jersey

Abstract. Recently, it was proposed (Baum, 1990 and Martin et al., 1990a, 1990b) that the southern ocean should be fertilized with iron to stimulate biological productivity, thus enhancing the flux of organic carbon from surface to depth, thereby lowering the concentration of inorganic carbon in surface water and in turn the atmospheric CO_2 concentration. We explore the possible impact of a hypothetical iron fertilization on atmospheric CO_2 levels during the next century using a high-latitude exchange/interior diffusion advection model. Assuming as an upper-limit scenario that it is possible to stimulate the uptake of the abundant nutrients in the southern ocean, the maximum atmospheric CO_2 depletion is 58 ppm after 50 years and 107 ppm after 100 years. This scenario requires completely effective Fe fertilization to be carried out over 16% of the world ocean area. Sensitivity studies and comparison with other models suggest that the errors in these limits due to uncertainties in the transport parameters, which are determined by calibrating the model with radiocarbon and validated with CFC-11 measurements, range from -29% to +17%. If iron-stimulated biological productivity is halted during the six winter months, the additional oceanic CO_2 uptake is reduced by 18%. Possible changes in surface water alkalinity alter the result of iron fertilization by less than +9% to -28%. Burial of the iron-induced particle flux as opposed to remineralization in the deep ocean has virtually no influence on the atmospheric response for the considered time scale of 100 years. If iron fertilization were terminated, CO_2 would escape from the ocean and soon cancel the effect of the fertilization. The factors which determine the atmospheric CO_2 reduction most strongly are the area of fertilization, the extent to which biology utilizes the abundant nutrients, and the magnitude of future CO_2 emissions. The possible effect of fertilizing the ocean with iron is small compared to the expected atmospheric CO_2 increase over the next century, unless the increase is kept small by means of stringent measures to control CO_2 emissions.

INTRODUCTION

The continuous increase of the atmospheric CO_2 concentration, caused by burning of fossil fuels and deforestation, is expected to have a major and probably undesirable impact on the future climate of the Earth. The control of future atmospheric CO_2 levels has thus become an important issue. Recently the idea was brought forward to fertilize large ocean areas with iron to decrease atmospheric CO_2 [Baum, 1990; Martin et al., 1990a, 1990b; W. Booth, Ironing out 'greenhouse effect'; fertilizing oceans is proposed to spur algae, Washington Post, p. A1, May 20, 1990].

The ocean largely controls atmospheric CO_2 concentration. The equilibrium partial pressure of CO_2 in seawater (pCO_2) is directly related to the concentration of dissolved inorganic carbon (ΣCO_2). In typical surface waters, ΣCO_2 is depleted by 10-20% relative to the deep sea, because carbon is continuously being exported to deeper layers by a flux

of biogenic particles, acting as a biological carbon pump. In many oceanic areas, biological productivity is limited by the nutrients phosphate and nitrate, resulting in near-zero nutrient concentrations, but in high-latitude surface waters, particularly in the southern ocean, the concentration of these nutrients remains relatively high throughout the year. Martin and Fitzwater [1988], Martin and Gordon [1988], Martin [1990], and Martin et al. [1989, 1990a, 1990b] have demonstrated, using sophisticated analytical methods, that in these regions the iron concentration in surface water is very low. They have interpreted the low abundance of iron and the results of their iron enrichment experiments as strong evidence that in these regions the biological production is limited by iron. They based their hypothesis on the increase of chlorophyll a concentration in bioassays with iron added in nanomolar concentrations, compared to controls without additional iron. It has been suggested, following the argument of Martin et al., that fertilizing the ocean with iron could be a means to control the atmospheric CO_2 increase [Baum, 1990; Martin et al., 1990a, 1990b]. The fertilization would, by enhancing biological productivity, lead to an increased particulate flux of carbon out of the surface ocean, and in this way provide a short circuit from surface to deep waters, lower the surface concentration of inorganic carbon, and consequently draw down atmospheric CO_2. Since the ratio of Fe to C incorporated by plants is rather low, between 1:10,000 and 1:100,000, a relatively modest amount of iron would be required. A problem, which we do not consider here, might be to find a suitable chemical form for dosing the iron (which is a very reactive element) in a bioavailable form.

The hypothesis that iron is the ultimate limiting nutrient is still highly controversial. De Baar et al. [1990] concluded, from shipboard experiments with water from the Weddell and Scotia seas, that iron, although enhancing the productivity, is not the productivity-limiting factor. Banse [1990, 1991] and Dugdale and Wilkerson [1990] found in their reanalysis of the data of Martin et al. that the specific algal growth rate (or cell division rate) and the specific uptake rate of nitrate were not affected by the added iron in the experiments of Martin et al. They concluded that the influence of added iron is on the loss terms rather than on the growth of chlorophyll a under the specific experimental conditions. This is what might enable phytoplankton mass to accumulate in the experimental bottles. Biological productivity may be limited by factors other than iron. Measurements of B. G. Mitchell and O. Holm-Hansen (Observations and modeling of the Antarctic phytoplankton crop in relation to mixing depth, submitted to Deep Sea Research, 1990) in the Brainsfield Strait and of Dugdale and Wilkerson [1990] in the Scotia and Ross seas indicate that the zooplankton grazing rates in these regions are high

and may therefore act as a control on phytoplankton productivity. Furthermore, deepening of the mixed layer by frequent storms in the southern ocean may result in light limitation for algal growth (B. G. Mitchell and O. Holm-Hansen, submitted manuscript, 1990). In spite of this controversy about the actual role of iron, we will for this paper adopt the hypothesis that the biological productivity in phosphate- and nitrate-rich waters can be enhanced by iron in some suitable chemical form until the concentrations of N and P are reduced to near-zero values.

Earlier studies have demonstrated that changes in biological productivity and the export of carbon in the southern ocean may lead to alterations of the atmospheric CO_2 content of about 100 ppm [Knox and McElroy, 1984; Sarmiento and Toggweiler, 1984; Siegenthaler and Wenk, 1984]. It would take several centuries to achieve the new equilibrium [Wenk and Siegenthaler, 1985]. In a previous paper [Joos et al., 1991] we have estimated the transient response of the carbon system to hypothetical iron fertilization scenarios. In this paper, sensitivity studies are presented to evaluate the importance of the different processes and to estimate the errors involved with the model assumptions. We will not consider any ecological effects of iron fertilization, which might be serious and which seem virtually impossible to assess presently, considering the very limited knowledge of the factors regulating marine ecosystems.

MODEL DESCRIPTION AND DETERMINATION OF TRANSPORT PARAMETERS WITH RADIOCARBON AND CFC-11

To address the potential of the ocean for enhanced removal of atmospheric CO_2, we use the high-latitude exchange/interior diffusion-advection model (HILDA) originally constructed by G. Shaffer and J. L. Sarmiento (Biogeochemical cycling in the global ocean 1: A new analytical model with continuous vertical resolution and high-latitude dynamics, unpublished manuscript, 1991) and used by U. Siegenthaler and F. Joos (Studying the anthropogenic carbon cycle perturbations and oceanic tracers using a high-latitude exchange/interior diffusion-advection ocean model, submitted to Tellus, 1991) to study the anthropogenic perturbations of CO_2, ^{13}C, and ^{14}C. It includes two well-mixed surface boxes, in low (LS) and high latitudes (HS), a well-mixed high-latitude deep water box (HD), a diffusive interior deep water box, and a well-mixed atmosphere (Figure 1). Water transport in the ocean is described by four parameters: an eddy diffusivity K, an advective flux w (upwelling in the interior box), an exchange flux u between HS and HD, and an exchange flux q (constant with depth) between the HD and interior boxes (Table 1).

HILDA Model

Atmosphere

gl   gh

0

LS   HS

75
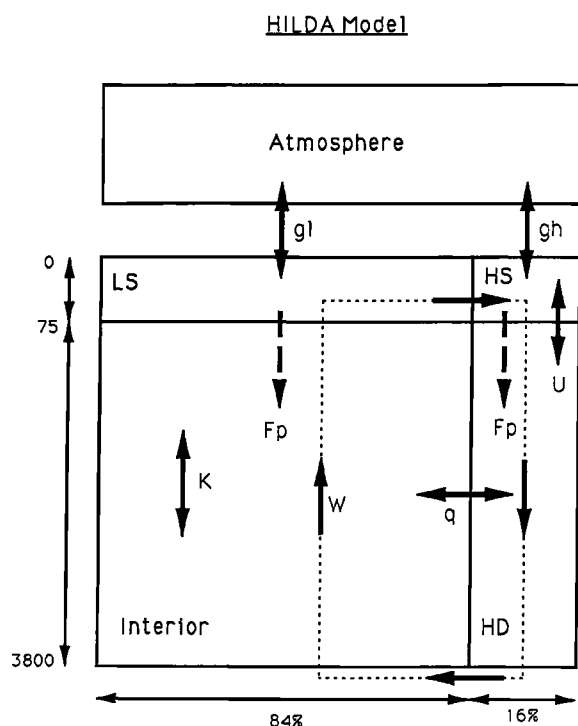
U

Fp   Fp

K

W   q

Interior   HD

3800

84%   16%

Fig 1. Structure of the HILDA model. Atmosphere, LS, HS, and HD are well-mixed reservoirs. The diffusive interior reservoir is numerically represented by 68 layers. The HS and HD boxes, representing the ocean south of 46°S, cover 16% of the ocean area. The depth of the model mixed layer (LS and HS boxes) is 75 m; the total depth of the ocean is 3800 m. Dashed arrows show particle fluxes (Fp); solid arrows show transport by gas exchange (gl, gh), diffusion (K), advection (w), and water exchange (u, q).

All transport parameters are determined such that the model reproduces the interior oceanic distributions of natural, steady state ^{14}C as well as of bomb-produced ^{14}C at the time of the Geochemical Ocean Sections Study (GEOSECS) survey (1974). To match these criteria, the eddy diffusivity, which in this simple model summarizes vertical transport on very large horizontal scales, requires larger values near the surface than at depth. Physically, this can be understood as parameterizing the effect of vertical mixing by wind and convective overturning and exchange by advection, all of which are much stronger in the uppermost layers than in the deep ocean. Furthermore, neutral (isopycnal) surfaces, along which transport and mixing preferentially occur, are more steeply inclined near the surface, thus giving a larger vertical component. This and other model features are discussed in detail elsewhere (Siegenthaler and Joos, submitted manuscript, 1991).

In the HILDA model the high-latitude surface (HS), originally chosen to represent water colder than 5°C, covers 16% of the world ocean area. Here we concentrate on the southern ocean, as it represents by far the largest pool of nutrient-rich surface water. We use phosphate to determine the extent of nutrient-rich waters. Oceanic surface phosphate concentrations range from 0 to about 2 mmol m^{-3}. The southern ocean's (>30°S) water volume in the depth range 0 - 75 m with >1.0 mmol m^{-3} phosphate amounts to 15.8% of the world ocean volume in the same depth range, and its average phosphate content is 1.63 mmol m^{-3}, based on global phosphate maps produced by S. Levitus and R. G. Najjar (personal communication, 1990); thus the 16% area of the world ocean covered by the HS-HD boxes represents the area of phosphate-rich surface water in the southern ocean. This fraction roughly corresponds to the ocean south of 46°S. We assume that the whole high-latitude surface region (HS) is fertilized by iron in such a way that its phosphate concentration decreases, due to the enhanced biological activity, by 1.5 mmol m^{-3}.

In the HILDA model the high-latitude ocean is represented by two well-mixed boxes. Representing the deep high-latitude ocean by one mixed box is obviously very coarse, but it is difficult to find a more realistic representation without abandoning the concept of a simple model. As the transport in high-latitudes is essential for the problem considered here, it is important to verify the model in this respect, which can be done by means of time-dependent tracers. In the calibration procedure the value of u, the exchange parameter between the HS and HD box, was determined by fitting the estimated preindustrial ^{14}C concentration in the high-latitude surface box as well as the observed high-latitude surface and deep ocean ^{14}C concentration in 1974, the time of the GEOSECS survey, and the observed global oceanic bomb radiocarbon inventory in 1974 [Broecker et al., 1985]. By 1974, large amounts of radiocarbon from the bomb tests in the 1950s and 1960s had penetrated into the ocean. No suitable measurements exist for the prebomb radiocarbon concentration in the deep southern ocean; thus we could not prescribe this concentration for the HD box. For this reason we also abstained from prescribing a separate bomb radiocarbon inventory for the high latitudes.

The model-calculated inventory of bomb ^{14}C in the HS and HD boxes (8.7×10^9 atoms cm^{-2}) is higher than the average value of 4.6×10^9 atoms cm^{-2} for the 17 stations south of 46°S (representing approximately the low- to high-latitude limit in our model) listed by Broecker et al. [1985]. However, the estimated average inventory has a large error, because the bomb signal is not easy to discern from the natural ^{14}C background and data in the southern ocean are scanty, especially from prebomb time. Also, bomb

TABLE 1. Model Parameters

Parameter	Description	Value
K	Eddy Diffusity in interior box, $m^2\ yr^{-1}$	$K=465 + 7061 \times exp(-(z-75\ m)/253\ m)$
gl,gh	Gas exchange rate for low- and high-latitude ocean at 280 ppm	$15.1\ mol\ m^{-2}\ yr^{-1}$
w	Upwelling velocity in interior box	$0.44\ m\ yr^{-1}$ (4.24 Sv)
u	Exchange flux HD <-> HS	$38\ m\ yr^{-1}$ (69.8 Sv)
q	Exchange coefficient of Interior with HD box	$0.00238\ yr^{-1}$ (85.5 Sv)
Aoc	Ocean surface area	$3.62 \times 10^{14}\ m^2$
h_s	Depth of mixed layer	75 m
h_{oc}	Average depth of ocean	3800 m
af	Fraction of ocean surface covered by HS box	0.16
$R_{C:P}$	Redfield ratio between carbon and phosphate	130
$R_{A:P}$	Redfield ratio between alkalinity and phosphate	0
τ	Time constant for particle flux	5 days
$\delta P_{HS}*$	Prescribed phosphate perturbation in HS box	$-1.5\ mmol\ m^{-3}$
$\delta P_{LS}*$	Prescribed phosphate perturbation in LS box	$0.0\ mmol\ m^{-3}$

inventories south of 46°S exhibit considerable variability, with a systematic southward decrease. Furthermore, the method by which Broecker et al. determined the bomb ^{14}C inventories may have led them to miss artificial ^{14}C that penetrated all the way down to the bottom. Therefore, we have also considered existing CFC data to further constrain the HILDA model.

Atmospheric concentrations of CFC-11 and CFC-12 have increased since about 1940. In the last few years, CFCs have been measured intensively in the ocean, and we have therefore calculated high-latitude ocean inventories for these tracers with the HILDA model. CFC data are easier to interpret than ^{14}C observations, as there is no natural background; furthermore, the relative analytical precision is better than that for bomb ^{14}C. CFC concentrations have been measured on several expeditions in the southern ocean. During the 1983-1984 AJAX experiment in the Atlantic Ocean, CFCs were measured between 5°N and 70°S along the 0° meridian and between 0° and 55°W along approximately 60°S [Weiss et al., 1990; Warner, 1988]. The average depth-integrated inventory of CFC-11 from the 63 AJAX stations south of 46°S is about 2000±100 nmol m^{-2}. In the Pacific Ocean, the National Oceanic and Atmospheric Administration Pacific Marine Environment Laboratory (NOAA-PMEL) measured CFCs down to 58°S between 150°W and 170°W during 1984; the corresponding average inventory is 1800 - 1900 nmol

m^{-2} (R. H. Gammon and D. Wisegarver, personal communication, 1990). During the 1985 Wilkesland experiment in the Pacific, CFCs were measured at 22 stations between 55°S and 70°S, 145°E and 165°E (R. F. Weiss and M. J. Warner, personal communication, 1990). The mean area- and depth-weighted inventory (taking the relative areas of 5° latitude bands of the Pacific Ocean [Levitus, 1982] as areal weights) is 2140 nmol m^{-2}. From these data sets, we estimated a CFC-11 inventory of 1950±550 nmol m^{-2} for the ocean south of 46°S in 1984. From measurements at the beginning of 1990 by NOAA-PMEL (J. L. Bullister, personal communication, 1990) in the Pacific Ocean on the same track as their 1984 cruise, a CFC-11 inventory of 2500 nmol m^{-2} for the 14 stations south of 45°S was obtained.

For calculating model inventories, we prescribed the observed southern hemisphere CFC-11 concentration (M. J. Warner, personal communication, 1990) for the atmosphere. Solubility constants were taken from Warner and Weiss [1985]. Gas exchange velocities were calculated from the formulation given by R. Wanninkhof (Relationship between wind speed and gas exchange over the ocean, submitted to Journal of Geophysical Research, 1991) for long-term average wind speeds; we have used an average wind speed of 7 m s^{-1}. The high-latitude inventory obtained for 1984 is 1976 nmol m^{-2}. Thus, the model result agrees well with the estimated actual inventory. For 1990 the model's inventory is 3097 nmol m^{-2},
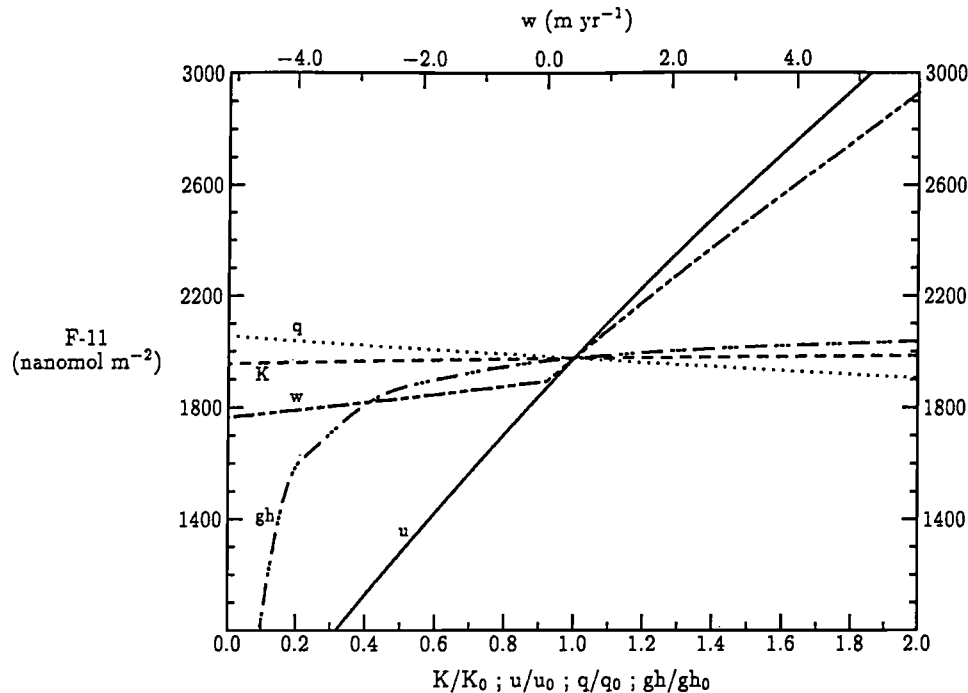
Fig. 2. Sensitivities of high-latitude inventory of CFC-11 (January 1, 1984) to variations in transport parameters. The standard values of the parameters indicated by the subscript 0 are given in Table 1. Negative w corresponds to downwelling in the interior and upwelling in the high-latitude ocean. The sensitivity of the high-latitude CFC-11 inventory to changes in the low-latitude gas exchange velocity is small (not shown).

somewhat high compared with the NOAA-PMEL observation of 2500 nmol m^{-2} along 150°-170°W. From 1984 to 1990 the NOAA-PMEL inventory went up by only 600-700 nmol m^{-2}, whereas the model inventory increased by 1100 nmol m^{-2}. The fact that the NOAA-PMEL inventory in 1984 is lower than the inventory obtained from AJAX and the Wilkesland experiment suggests that the ventilation rate at the location of the NOAA-PMEL measurements may be relatively low; thus the CFC-11 increase rate for the whole southern ocean may be underrepresented in the NOAA-PMEL data. On the other hand, the difference between the observed increase in CFC-11 and the model increase may also be due to the highly simplified representation of transport in HILDA.

To determine the sensitivity of the predicted CFC-11 inventory to changes in the model parameters, we carried out a series of runs in which parameters were varied individually, usually by up to a factor of 2 times its standard value (see Figure 2). The most important model parameter is u, i.e., the vertical exchange between the two high-latitude boxes. The value of u is well constrained by the high-latitude CFC-11 inventory, which is sensitive to u but relatively insensitive to the other parameters. The error in the CFC-11 inventory of ±550 nmol

m^{-2} results in an error of ±40% for u (Figure 2). The standard model parameters we chose for HILDA thus seem to be supported by the CFC data. The bomb ^{14}C discrepancy must, however, be studied further.

INCLUDING CARBON IN THE MODEL

For studying the effect of enhanced biological production on future CO_2 levels we chose a perturbation approach. Ice core measurements indicate that the atmospheric CO_2 concentration varied by less than ±5 ppm during the 1000 years prior to the beginning of industrialization [Siegenthaler et al., 1988], implying that the carbon cycle was approximately in steady state before 1800. Therefore, we assume that the natural carbon cycle continues to operate unchanged, an assumption made thus far by virtually all modeling studies of the anthropogenic CO_2 increase. This allows us to simplify the procedure considerably. Instead of simulating the whole natural carbon cycle, we only consider its changes, caused by anthropogenic CO_2 emissions, i.e., fossil fuel burning and land clearing, and by a hypothetical fertilization of the ocean with iron.

To calculate the particle flux which might result from iron fertilization, we take phosphate as a guide. Once phosphate is depleted in the surface water, it becomes the limiting factor for biological production; hence fertilization with iron no longer has any effect. As an upper limit scenario it is assumed that it is possible to completely deplete phosphate in that part of the southern ocean represented by the HS box of our model. Perturbation particle fluxes (carrying C and P) are included in the model equations. The particles leaving the surface are remineralized completely in the deep water column. We assume that in the interior reservoir the particle remineralization decreases exponentially with depth, with a depth scale of 1160 m (G. Shaffer and J. L.Sarmiento, Biogeochemical cycling in the global ocean 1: A new analytical model with continuous vertical resolution and high-latitude dynamics, unpublished manuscript, 1991). For the present ocean, the perturbation particle flux and the perturbation of the phosphate concentration are zero by definition. For simulating a full fertilization by iron, we prescribe a decrease of the P concentration of -1.5 mmol m^{-3} in the HS box and of 0 mmol m^{-3} in the LS box. This corresponds to a nearly total depletion of P in the southern ocean and to an unchanged low concentration in lower latitudes. The particle fluxes necessary to achieve these perturbations are calculated by means of a phosphate balance in each surface box. The calculated phosphate perturbation in surface box i, δP_i, is forced toward the prescribed values δP_i^* of -1.5 and 0 mmol m^{-3} (high and low latitudes), setting the particle flux F_i equal to

$$F_i(particle) = 1/\tau \times (\delta P_i - \delta P_i^*) \qquad (1)$$

where τ is a time constant. As a standard value for τ, 5 days was chosen, forcing the model rapidly to the prescribed value of δP_i^*. Multiplying the resulting P flux by the Redfield ratio C:P = 130, i.e., the ratio at which the two elements are incorporated into organic particles, yields the carbon flux. This scenario obviously provides a maximum upper limit, since other factors such as mixed layer depth and light supply, temperature, and the ecosystem behavior probably interfere long before phosphate is depleted. Furthermore, it seems hardly feasible to spread iron in a suitable chemical form, continuously over many decades, over an area of 16% of the world ocean.

As the aqueous carbonate chemistry, which governs the relation between changes of pCO_2 and ΣCO_2, is nonlinear with respect to concentrations, the effectiveness of the iron fertilization depends upon the atmospheric and oceanic CO_2 concentrations. To study these factors, three different scenarios of atmospheric CO_2 are used. In the "preindustrial scenario," pCO_2 in surface waters and in the atmosphere is assumed to have the preindustrial value

of 278.3 ppm [Neftel et al., 1985; Friedli et al., 1986]. In the two other scenarios, atmospheric CO_2 concentration is prescribed until 1990 using the results of ice core measurements and direct atmospheric observation [Neftel et al., 1985; Friedli et al., 1986; Keeling et al., 1989] in the way described by Siegenthaler and Oeschger [1987]. In the "constant emission scenario" the annual emission to the atmosphere after 1990 is fixed at the model-determined value of 6.15 Gt C yr^{-1} in 1990. In the "business-as-usual" scenario the annual emission is prescribed according to the IPCC business-as-usual scenario [Intergovernmental Panel on Climate Change (IPCC), 1990] according to which emissions grow linearly to a value of 22.4 GtC yr^{-1} in 2100. In both of the latter scenarios, iron fertilization is started in 1990. In the surface water, carbonate chemistry is taken into account in the gas exchange equations using the chemical equilibrium equations and constants given by Peng et al. [1987], assuming everywhere a salinity of 35o/oo and an alkalinity of 2300 µeq kg^{-1}, a temperature of 19.9°C in the LS and -0.22°C in the HS box, and that in preindustrial time the two surface boxes were in equilibrium with an atmosphere of 280 ppm. As a standard, alkalinity changes are neglected, as biogenic particles carry relatively little carbonate in the southern ocean, and the effect of carbonate uptake on alkalinity is approximately canceled by uptake of NO_3^-. We explored the effect of including alkalinity in some sensitivity runs, as mentioned below.

RESULTS

The change in atmospheric CO_2 resulting from the hypothetical iron fertilization for the business-as-usual and the constant emission scenarios is shown in Figure 3a. Without fertilization, atmospheric CO_2 increases from 355 ppm in 1990 by 146 ppm in 50 years and by 417 ppm in 100 years for the business-as-usual scenario. When iron fertilization is started, an additional particle flux out of the HS box is stimulated. Its size is approximately constant at 5.46 Gt C yr^{-1} after an initial peak in the first year. This flux leads to a massive decrease in the high-latitude surface pCO_2 (Figure 3b), and to an increased uptake of atmospheric CO_2 (Figure 3c). The atmospheric CO_2 now increases by only 88 ppm in 50 years and by 310 ppm in 100 years. After 100 years, the additional CO_2 flux from the atmosphere into the high-latitude ocean due to iron fertilization is 2.64 Gt C yr^{-1}, partly balanced by a reduction of 0.52 Gt C yr^{-1} in the low-latitude CO_2 uptake. This results in a net annual oceanic uptake of 2.12 Gt C yr^{-1} due to iron fertilization (Figure 4). At year 100 (A.D. 2090), the export of 5.46 Gt C yr^{-1} of particulate carbon out
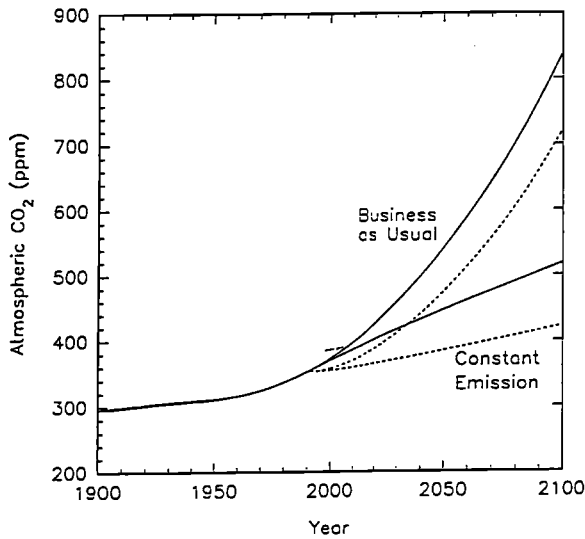
Fig. 3a. Future atmospheric CO2 concentration in the business-as-usual and constant emission scenarios. The solid lines are our predictions without iron fertilization; the dashed lines show what might occur with iron fertilization.
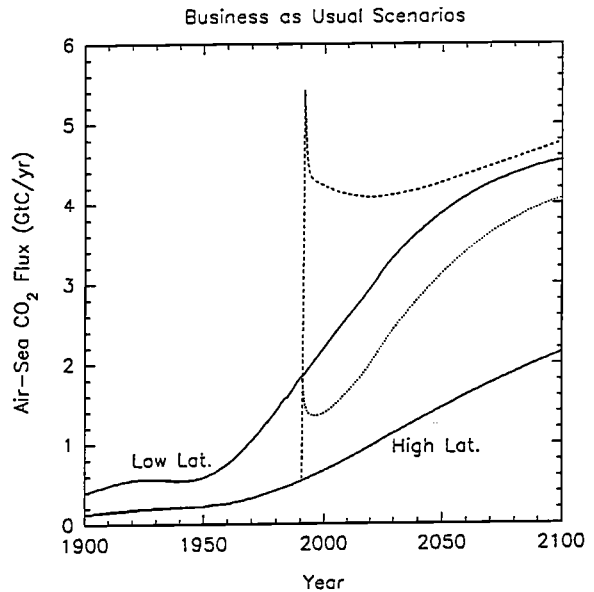

Business as Usual Scenarios

Fig. 3b. The air-sea CO2 difference of the iron-fertilized business-as-usual scenario (dashed lines) and the nonfertilized business-as-usual scenario (solid lines).

of the high-latitude surface box is balanced by an inflow of 2.64 Gt C yr^{-1} from the atmosphere due to iron fertilization alone, further by a reduction in the export of excess CO2 to the deep sea of 2.87 Gt C yr^{-1} and by a reduction of the inflow from the LS box

Fig. 3c. Air-sea flux of CO2 for unfertilized (solid line) and fertilized business-as-usual scenarios. The dotted line is the low-latitude flux in the fertilized scenario; the dashed line is the high-latitude flux in the fertilized scenario. All fluxes are into the ocean. Figures 3a and 3b are taken from Joos et al. [1991].
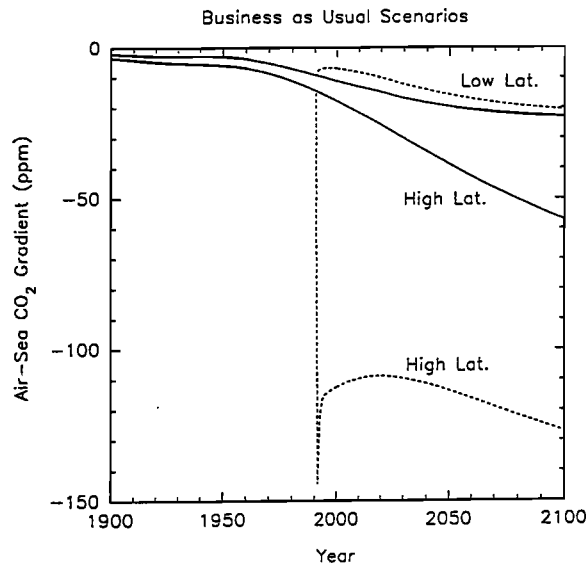
to the HS box by the advective flux w of 0.04 Gt C yr^{-1} (Figure 4).

In order to gain some insight into the relation between high-latitude particle flux, ocean circulation, and atmospheric CO2, we first consider the system HS plus HD boxes isolated from atmosphere and low-latitude ocean. After achieving a steady state, the particulate carbon transport F_C to depth is balanced by an equal upward transport of dissolved carbon by the water exchange flux u, and at the same time, it is related to the corresponding quantities for phosphate by the Redfield ratio $R_{C:P}$:

$$F_C = u \times R_{C:P} \times (P_{HD} - P_{HS}) \qquad (2)$$

$$F_C = u \times (\Sigma CO_{2;HD} - \Sigma CO_{2;HS}) \qquad (3)$$

where P is the phosphate concentration (note that the first equation also holds if an atmosphere is added). This relation shows that the depletions of phosphate and carbon in the surface box, compared to the deep box, are always in a fixed proportion (in this two-box consideration). In a second step, we now "switch on" the exchange with the atmosphere and the low-latitude ocean. CO2 from the low latitudes and from the atmosphere will invade the HS box via gas exchange. If the mixing rate u between surface and deep ocean is slow, this additional CO2 will essentially remain in the surface box, reducing the air-sea CO2 gradient,
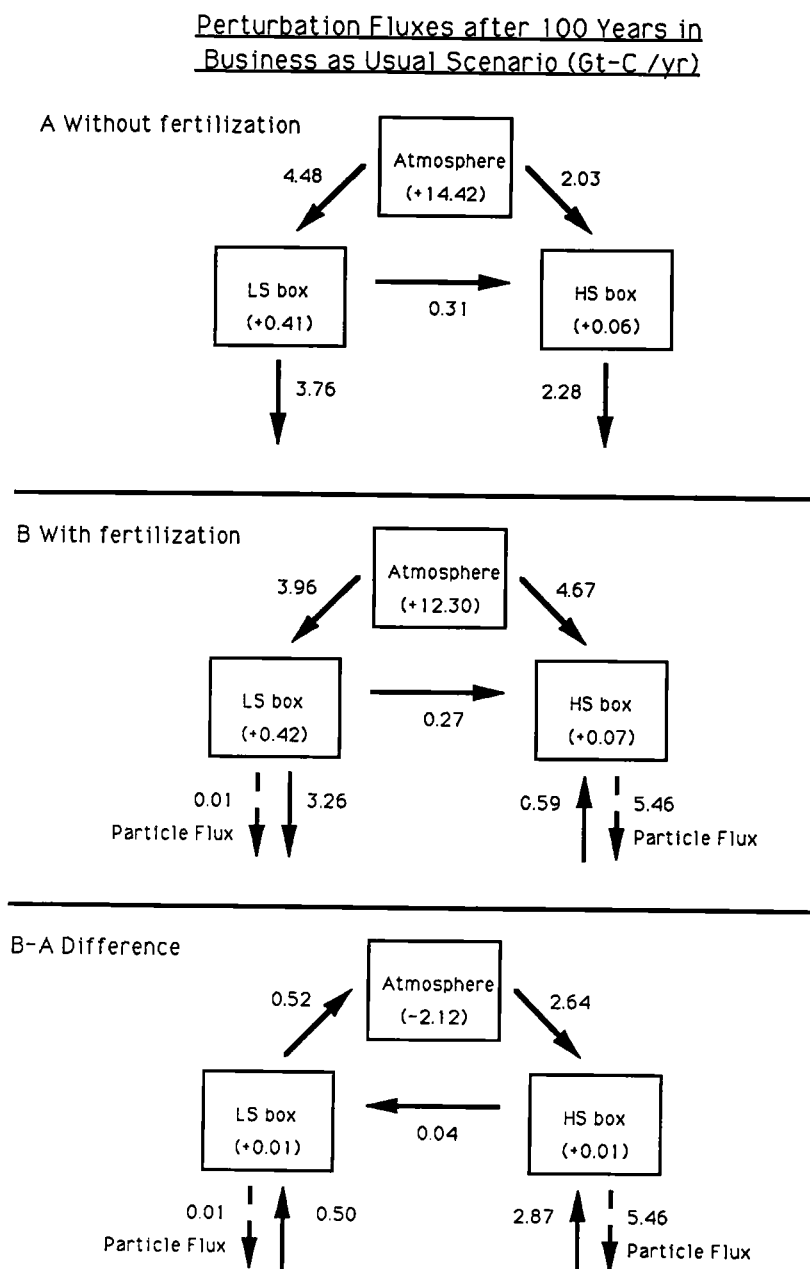
Perturbation Fluxes after 100 Years in Business as Usual Scenario (Gt-C /yr)

A Without fertilization

B With fertilization

B-A Difference

Fig. 4. Net fluxes in Gt C yr^{-1} between the different reservoirs for the business-as-usual scenario at year 100 (A.D. 2090). Solid lines represent transport via gas exchange and water transport; dashed lines represent transport by particles. Numbers in parentheses give change in reservoir size.

and the effect of iron fertilization will be small. For a large u the CO_2 imported from the atmosphere into the HS box is transported quickly to the deep ocean, and the CO_2 reduction caused by iron fertilization will be significant. This shows that it is, in principle, not the particle flux but the water circulation which transports the additional CO_2 to depth. What the

particle flux does is to draw down pCO_2 in high-latitude surface water, which provides the cause for the enhanced air-to-sea flux.

Because the mass of phosphate is conserved and the volume of the deep sea is much larger than the volume of the HS box, the absolute value of the P perturbation in the HD box is much smaller than in the

TABLE 2. Projected Changes in Atmospheric CO_2 Partial Pressure (ppm) After 100 Years Resulting From Various Scenarios

Scenario*	A Unfertilized	B Fertilized	(B-A) Effect of Fertilization	Ratio to Standard Scenario
"Standard" scenario, business-as-usual	417	310	-107	1.00
Effect of CO_2 level				
Initialized at preindustrial level	0	-59	-59	0.55
Constant emission	151	61	-90	0.84
Effect of alkalinity				
A:P Redfield ratio = -17	417	300	-117	1.09
A:P Redfield ratio = +40	417	340	-77	0.72
Effect of particle burial				
100% of P and C flux buried	417	310	-107	1.00
10% of C flux buried	417	305	-112	1.05
100% of C flux buried	417	259	-158	1.48
Effect of light				
No light in winter	417	329	-88	0.82

*Description of different scenarios given in text.

HS box. Thus the particle flux is approximately given by the prescribed surface P depletion, the Redfield ratio between P and C, and the surface to deep exchange (equation (2)).

The effect of carbonate chemistry is illustrated by the three different scenario calculations (Table 2). For the preindustrial scenario, iron fertilization reduces atmospheric CO_2 concentration by 59 ppm after 100 years. The atmospheric increase in CO_2 is lowered in the constant emission scenario by 90 ppm and in the business-as-usual scenario by 107 ppm after 100 years of iron fertilization. The reason for these differences can be understood by considering that pCO_2 depends in an nonlinear way on ΣCO_2. The change in pCO_2 for a given reduction of ΣCO_2 due to iron fertilization is larger, the higher the CO_2 level (Figure 5). Thus the effect of iron fertilization is larger for scenarios which include realistic emissions of anthropogenic CO_2 than for a preindustrial scenario.

Besides carbon and phosphate, sinking particles transport alkalinity. The generalized Redfield ratio $R_{A:P}$, which relates the transport of alkalinity and P by the sinking particles, depends on the ecosystem composition. Its average is not well known for the high-latitude ocean. However, a range of $R_{A:P}$ can be estimated. The upper limit is found by assuming that as much carbonate formation occurs in high latitudes as is estimated for the low latitudes and used in other modeling studies [Sarmiento and Toggweiler, 1984; Siegenthaler and Wenk, 1984]; the lower limit is determined by assuming that no $CaCO_3$ formation occurs and that alkalinity is only affected by the uptake of NO_3^-. This yields a range for $R_{A:P}$ of +40 to -17. The assumed perturbation of phosphate in the HS box of -1.5 mmol m^{-3} results therefore in an alkalinity change in the HS box of -60 to 25.5 mmol m^{-3}. Relative to the case when $R_{A:P} = 0$, for 100 years of iron fertilization the additional CO_2 uptake of 107 ppm in the business-as-usual scenario is increased by 10 ppm when $R_{A:P} = -17$ but reduced by 30 ppm when $R_{A:P} = +40$ (see Table 2).

To explore how the model results depend on the model assumptions, and to better understand the processes involved, a number of sensitivity studies were carried out using the preindustrial scenario. Figure 6 shows the sensitivity of the atmospheric CO_2 change after 100 years to changes in the model parameters, varying one particular parameter while keeping all others fixed. Note that changing the model
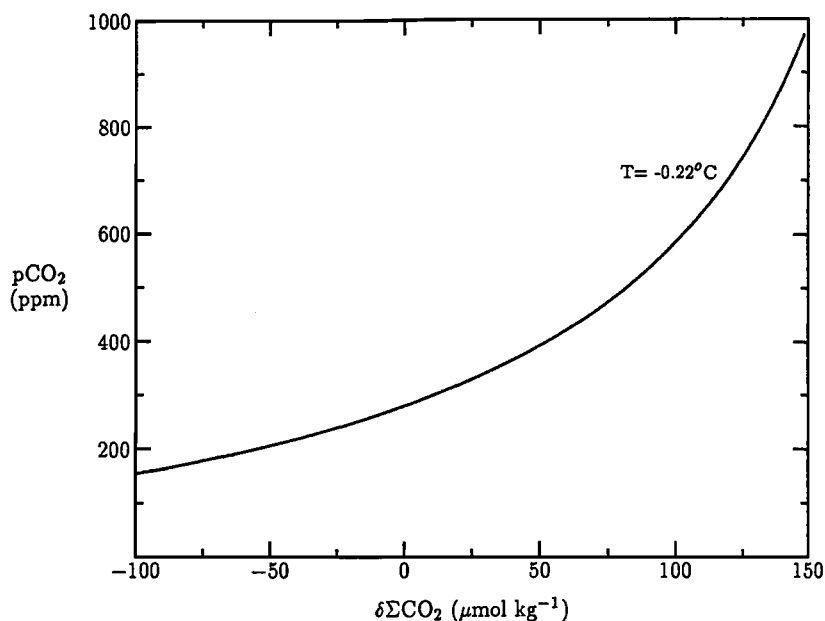
Fig. 5. Dependence of the partial pressure of CO_2 (pCO_2) on the perturbation of the concentration of total inorganic carbon ($\delta\Sigma CO_2$) in high-latitude surface water. $\delta\Sigma CO_2$ denotes the deviation from the preindustrial equilibrium. The relation was calculated using the carbonate equilibrium scheme given in Peng et al. [1987], with the following "preindustrial" values: ΣCO_2= 2125 μmol kg^{-1}, alkalinity of 2300 μmol kg^{-1}, salinity of 35o/oo, and temperature of -0.22°C. This figure is taken from Joos et al. [1991].

parameters arbitrarily may violate the restrictions we have imposed when calibrating the model. When varying one parameter in a significant way, a new calibration should in principle be carried out, adjusting also other parameters. Figure 6 therefore gives sensitivities in this restricted sense only.

Despite the fact that the effect of iron fertilization depends strongly on the prescribed CO_2 levels, the model behaves almost linearly for a given scenario within the range of parameter values shown in Figure 6a. This means that the carbonate chemistry equations are locally quite linear. This allows us to find a scaling factor, which is a function of time, to use to calculate from the sensitivity experiments with the preindustrial scenario the sensitivity for the two other scenarios. This factor, determined after 100 years, is 1.81 for the business-as-usual scenario and 1.52 for the constant emission scenario. This relationship holds within ±6% for the parameter variations shown in Figure 6a. The same scaling factors apply also for variations in the transport parameters (Figures 6b and 6c) as long as the oceanic CO_2 uptake for the unfertilized scenario is not significantly altered. This is true except for extreme parameter values.

The most important parameters in determining the atmospheric response to iron fertilization are the area fraction of the high-latitude ocean, af (which we have chosen as 16% of the world ocean based on the observed phosphate distribution), and the prescribed phosphate depletion in the high-latitude surface box (Figure 6a). These two parameters determine the maximal possible phosphate and carbon depletion in the surface ocean.

We consider now the effect of the transport parameters on the response to iron fertilization. Enhanced vertical mixing in high latitudes (u) results in a greater ΣCO_2 decrease in the HS box and, in turn, a larger atmospheric signal (Figure 6b). This is attributable to greater water exchange driving more imported CO_2 from the low-latitude ocean and the atmosphere to the deep sea. Increasing the gas exchange rate in high latitudes (gh) allows the high-latitude ocean to influence the atmospheric CO_2 more strongly (Figure 6c). Increasing the gas exchange rate (gl) or the vertical mixing (K) in low latitudes leads to more outgassing of CO_2 from the LS box and thus reduces the atmospheric perturbation (Figures 6b and 6c). Horizontal exchange in the deep ocean (q) is unimportant, since the mean perturbation of the CO_2 concentration at depth is very small (Figure 6b). With increasing w, the surface to deep exchange becomes more effective, and thus the effect of iron fertilization becomes larger.

From these sensitivity studies one can estimate the uncertainties of the iron fertilization effect attributable to uncertainties associated with transport parameters.
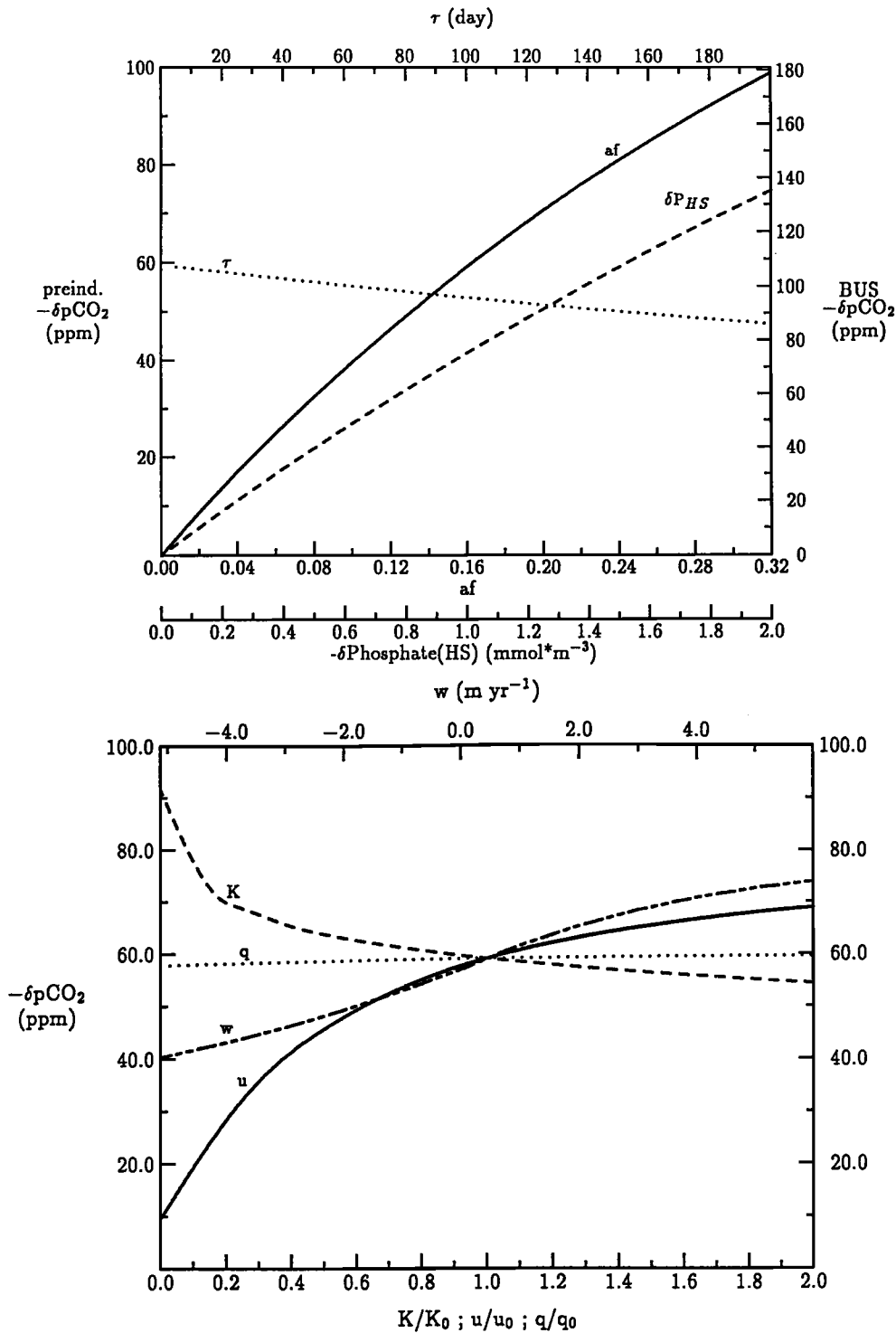
τ (day)

20   40   60   80   100   120   140   160   180

100 ── 180

                                                    160

80   af   140

                                    δP_{HS} 120

preind.   100   BUS
$-\delta pCO_2$ τ $-\delta pCO_2$
(ppm)   80   (ppm)

40   60

                                                    40

20   20

                                                     0
0.00 0.04 0.08 0.12 0.16 0.20 0.24 0.28 0.32
                        af

0.0 0.2 0.4 0.6 0.8 1.0 1.2 1.4 1.6 1.8 2.0
              $-\delta$Phosphate(HS) (mmol*m^{-3})

w (m yr^{-1})

        −4.0   −2.0   0.0   2.0   4.0

100.0 ── 100.0

80.0   80.0
          K

60.0   q   60.0

$-\delta pCO_2$
(ppm)   w

40.0   u   40.0

20.0   20.0

0.0 0.2 0.4 0.6 0.8 1.0 1.2 1.4 1.6 1.8 2.0
              K/K$_0$; u/u$_0$; q/q$_0$

Fig. 6. Sensitivity of the reduction in atmospheric CO2 after 100 years due to iron fertilization for the preindustrial scenario. Each parameter was varied while all others were held constant. The standard values of the parameters indicated by the subscript 0 are given in Table 1. The right axis in Figure 6a shows the derived difference in atmospheric CO2 between the unfertilized and fertilized business-as-usual scenario (BUS; see text for explanation). Note the different scale for w in Figure 6b.
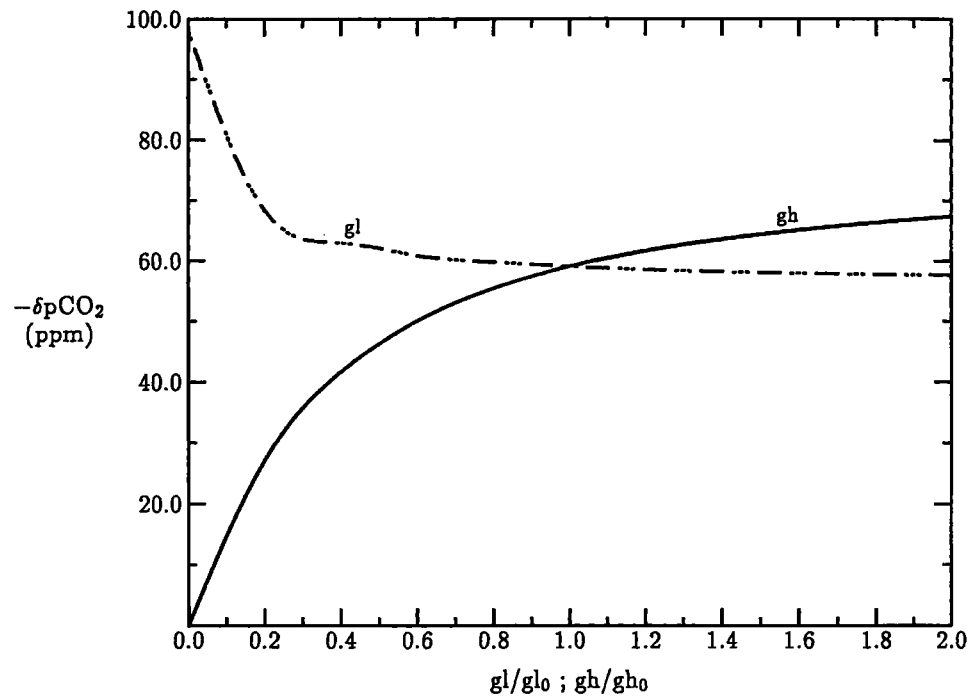
Fig. 6.   (continued)

The exchange parameter between the two high-latitude boxes, u, is constrained by the analysis of the CFC-11 inventory within ±40% of its standard value. As a conservative error estimate, we assume a similar uncertainty for the other transport parameters. In the HILDA model the vertical exchange due to water which is upwelling in the high latitudes and then transported again to depth as Antarctic Intermediate Water, as Antarctic Mode Water, or beneath the Antarctic's sea ice fringe is parameterized by u rather than by w. The advective flux w represents a thermohaline overturning, but does not account for the wind-driven upwelling in the southern ocean. Peng and Broecker [1991] estimated the flux of water upwelling in the southern ocean to be 17.4 sverdrups (Sv). Following Peng and Broecker, we choose a value of -2 m yr^{-1} as a lower limit for w, thus including the possible impact of wind-driven upwelling on w. Note that in the HILDA model all the water upwelling in the high latitudes (i.e., w< 0) is directed into the LS box. With this transport path, the surface to deep transport for CO_2 imported from the atmosphere and low-latitude ocean is less efficient, compared to a case where the upwelling water would be exported into the deep ocean (i.e., the HD box). Thus the chosen transport path for negative w reflects also a lower limit with respect to the atmospheric CO_2 reduction due to fertilization. Since the model behaves almost linearly, for a given scenario the errors resulting from each parameter can be superimposed. To calculate the total error of the atmospheric CO_2 reduction due to uncertainties in all transport

parameters we use Gauss' error propagation law (quadratic addition of the individual errors). With the assumed limits for the transport parameters, we obtain for the preindustrial scenario a range for the additional oceanic CO_2 uptake of 42 ppm to 69 ppm after 100 years, i.e., an error of -29% and +17% for the standard value of 59 ppm. The individual parameters contribute the following errors: u, -10.1 to 5.3 ppm; w, -9.8 to 6.2 ppm; gh, -9.0 to 4.6 ppm; K, -2.3 to 3.5 ppm; gl, -0.8 to 1.8 ppm; and q, -0.6 to 0.3 ppm.

The size of the additional particle flux out of the surface ocean is proportional to the prescribed phosphate depletion, the area of fertilization, and the exchange rate between the HS and the HD box (Figure 7, see also equation (2)). It is interesting that for upwelling in the high-latitude ocean (w<0) the particle flux increases with stronger upwelling (Figure 7) but the effect of iron fertilization on atmospheric CO_2 decreases (Figure 6b). This illustrates that the atmospheric response is not determined by the particle flux alone but by the interplay of circulation, gas exchange, and particle flux.

In order to be effective, the iron fertilization would have to be applied continuously every year; if fertilization were to be stopped, atmospheric CO_2 would increase at a rate faster than if there had been no fertilization, thereby forcing the atmosphere-ocean system to revert to its unfertilized state. This is illustrated in Figure 8, which shows the behavior of the atmospheric CO_2 concentration if iron fertilization is terminated after 20 or after 50 years.
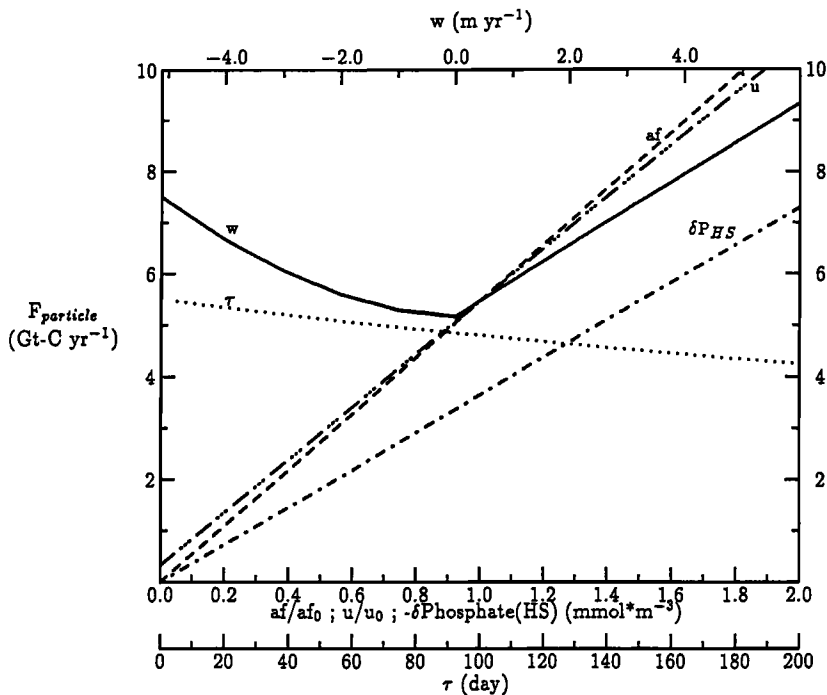
Part of the additional particle flux due to iron

Fig. 7. Sensitivity to relevant model parameters of the total particle flux (at year 100) out of the surface ocean stimulated by iron fertilization. Each parameter was varied while all others were held constant. The standard values of the parameters are given in Table 1. The particle flux is the same for all three scenarios. Note the different scale for w.

fertilization might be buried in sediments, or part of the additional new production might be transformed in long-lived dissolved organic matter with a breakdown rate of the order of 1/200 yr^{-1}, instead of sinking to the deep and remineralizing in 3-30 days [Legendre and Gosselin, 1989]. If all the additional particle flux caused by iron fertilization is removed from the ocean, the phosphate and carbon concentrations in the high-latitude deep box decrease by 0.71 mmol m^{-3} and 93 mmol m^{-3} after 100 years of fertilization relative to the scenario where all particles are remineralized in the deep ocean. The latter value is equal to the phosphate reduction times the C:P Redfield ratio ($R_{C:P}$=130). If burial is complete, less deep P and C are available for transport to the surface, thereby reducing the particle flux from approximately 5.5 Gt C yr^{-1} in the standard scenario to 3.0 Gt C yr^{-1}. However, the surface concentration of phosphate is prescribed; so ΣCO_2, related to phosphate by the Redfield ratio $R_{C:P}$, remains the same as in the standard scenario. Therefore atmospheric CO_2 is not affected by particle burial (see Table 2).

Carbon and phosphate may be remineralized at different rates in the water column and from the sediments. To account for this effect, we have performed a model run assuming that only carbon is buried in the sediment, but not phosphate. The

particle flux out of the surface ocean, which in this model is not limited by the carbon concentration, remains therefore the same, but the carbon transport from the deep to the surface is lower than in the standard experiment. If 10% of the additional carbon flux is buried, the difference relative to scenarios where all the particles are remineralized is less than 5.2 ppm after 100 years (Table 2). If 100% of the additional carbon flux is buried, then the difference relative to scenarios which include remineralization is 51 ppm (Table 2). However, this is an extreme scenario, and it is unlikely that the whole additional particle flux will be buried and that only carbon is removed, but not phosphate.

During the winter months there is no light in the high latitudes, and biological productivity is close to zero. To investigate light limitation, we carried out a run in which the particle flux was set equal to zero during 6 months of the year and calculated as usual (equation (1)) during the rest of the time, i.e., light limitation during summer, which might be important (B. G. Mitchell and O. Holm-Hansen, submitted mauscript, 1990), is not considered. In the business-as-usual scenario the additional oceanic uptake of CO_2 is lower by 10 ppm (17%) after 50 years and 19 ppm (18%) after 100 years compared to the scenario with continuous particle flux.

Remineralization of sinking particles uses oxygen. Sarmiento et al. [1988] show that the deep ocean
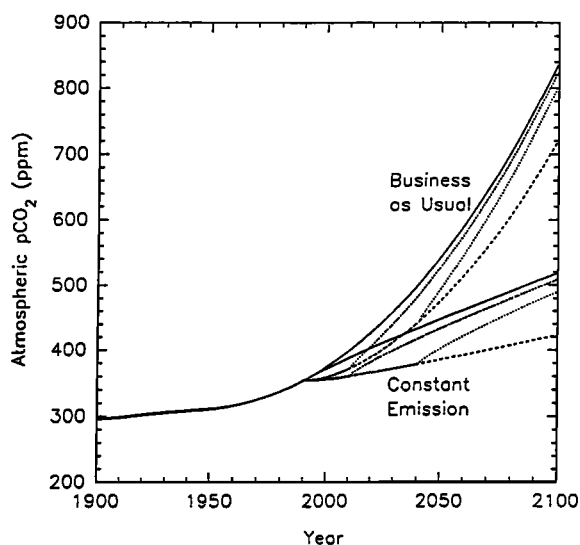
Fig. 8. The effect of stopping iron fertilization after 20 years (short-dashed line) and 50 years (dotted line) is depicted for the business-as-usual and constant emission scenarios. The solid line is the unfertilized scenario; the medium-dashed line is the scenario for continuous fertilization.

would finally become anoxic if all the nutrients in the high latitudes were consumed by biological production. Oxygen is related to P by a Redfield ratio (R_{O_2}:P). R_{O_2}:P is not known exactly. With R_{O_2}:P = -138, the classical value of Redfield, and with R_{O_2}:P= -169 [Takahashi et al., 1985] we calculated a depletion in the HD box in the range of 98 to 120 mmol m^{-3} after 100 years of iron fertilization. These values have to be compared to the oxygen concentration in the deep southern ocean, which is in the range of 160 to 240 mmol m^{-3} [Takahashi et al., 1981]. The additional oxygen depletion in the interior box is a strong function of depth, with near-zero values close to the LS box and comparable values as in the HD box at the bottom. The average depletion in the interior box is between 10 and 13 mmol m^{-3} after 100 years. The observed average oxygen concentration in the deep ocean is approximately 170 mmol m^{-3} [Takahashi et al., 1981]. Thus the deep sea would not become anoxic within 100 years. The relative reduction of the deep oxygen concentration in high latitudes is, however, not small. In reality the remineralization of the iron-induced particle flux would occur more locally, so that parts of the high-latitude deep ocean might become anoxic. To assess the problem of a possible anoxia of the deep ocean, a three-dimensional ocean model, with more realistic transport pattern than HILDA, has to be used.

DISCUSSION AND CONCLUSION

The magnitude and rate of the atmospheric decrease of CO_2 due to iron fertilization are governed by three transport processes: (1) an additional particle flux out of the southern ocean results in a decrease of ΣCO_2 and pCO_2 in the surface water; (2) the southern ocean communicates via gas exchange with the atmosphere and withdraws CO_2 from the atmosphere and the mid- and low-latitude surface ocean; and (3) the CO_2 withdrawn from the low-latitude ocean and from the atmosphere is transported to depth.

The relationship between the iron-induced CO_2 flux to the ocean and the additional particle flux depends on the overall transport pattern, e.g., on the water fluxes u and w. For instance, for a reversed advective water flux w, a given particle flux perturbation will have a different effect on atmospheric CO_2 than for the standard case. More generally, the biological carbon pump consists not only of the particle flux but of the interaction between particle flux, transport by water circulation, and atmosphere-ocean gas exchange.

The factors that most strongly influence the magnitude of the effect of a hypothetical iron fertilization are the size of the averaged phosphate depletion, the residence time of the phosphate- and carbon-depleted water at the surface (i.e., the size of the water flux from depth), and the CO_2 emission scenario. Considering the transport parameters, the model is most sensitive to the magnitude of the surface to deep exchange in high latitudes and the gas exchange in high latitudes. From our sensitivity studies with CFC-11 and from the model results of natural and bomb radiocarbon we conclude that the maximum error in the estimated CO_2 uptake due to an inappropriate choice of transport parameters is -29%/+17%. Peng and Broecker [1991] estimated the reduction of atmospheric CO_2 by iron fertilization to be 10±5% of the absolute concentration. According to Table 2 we get reductions of 21%, 18%, and 14% for the preindustrial, constant emission, and business-as-usual scenarios, which is more than indicated by Peng and Broecker. We can make a detailed comparison with their standard scenario, for which they get a reduction of 34 ppm after 100 years, while we get a decrease of 107 ppm for the business-as-usual scenario. The difference between the results can be explained as follows, based on our sensitivity analysis: 48 ppm can be attributed to the CO_2 level (they considered only a preindustrial scenario), and 20 ppm to a reduction of the area fraction from 16% to their choice of 10%. There remains a difference of only 5 ppm, which is well within the error bounds given above. It is obvious that the results of iron fertilization for the preindustrial situation are completely different than for realistic present and future CO_2 levels. The choice of the fertilized ocean

area is somewhat arbitrary; our choice of 16% of the world ocean corresponds, as explained above, to the part of the southern ocean region where phosphate is abundant. The fact that the deviation between our result and that of Peng and Broecker, which remains after correction for CO_2 concentration and fertilized area, is only 5 ppm indicates that the different transport schemes used have a minor influence on the final result.

The size of the particle flux is determined by the area of fertilization and by the degree to which biology is able to make use of the advected nutrients. For the prescribed scenarios a particle flux out of the high-latitude ocean of the order of 5 Gt C yr^{-1} was obtained. This can be compared to an estimate of the global particulate carbon flux to the deep sea of between about 4 Gt C yr^{-1} [Eppley and Peterson, 1979] and 7-13 Gt C yr^{-1} [Najjar, 1990].

All model assumptions were chosen in order to obtain an upper limit for the atmospheric CO_2 reduction. To be more specific, other possible limiting factors for biological production such as light and zooplankton grazing were completely ignored; we assumed that iron can be spread over an area of 16% of the ocean, such that iron is available in sufficient concentration, in suitable chemical form, permanently during 100 years. Our results indicate that even a totally effective iron fertilization of the whole southern ocean cannot avoid a future atmospheric CO_2 increase, not even for the unlikely assumption that emissions would not grow any more from 1990 on. For the business-as-usual scenario, we found for the next century a maximum possible reduction of the atmospheric CO_2 increase due to iron fertilization of 26%. The same reduction is 60% for the constant emission scenario. Thus, we conclude that the possible effect of iron fertilization on atmospheric CO_2 is only significant if the rate of atmospheric CO_2 increase is kept low by strict emission control measures.

The purpose of this study is to outline the magnitude of atmospheric CO_2 reduction attributable to a hypothetical stimulation of marine biological productivity. We cannot exclude that in our simple model some important processes are not correctly included. For example it is not possible at this time to assess the possible effect of dissolved organic matter [Legendre and Gosselin, 1989; Toggweiler, 1989]. Furthermore, it is as yet an open question if iron fertilization does indeed limit biological new production and transport of organic material out of the surface ocean. Our model results should therefore be considered as a sensitivity study rather than as an attempt to give a definitive answer. However, the calculations presented herein indicate that great efforts would be required to achieve even a modest effect on atmospheric CO_2 and that fertilization would need to be continued over an indefinite time. Otherwise, the sequestered CO_2 would escape again to the atmosphere, on a similar time scale as it was removed previously.

REFERENCES

Banse, K., Does iron really limit phytoplankton production in the offshore subarctic Pacific?, Limnol. Oceanogr., 35, 772-775, 1990.

Banse, K., Iron availability, nitrate uptake, and exportable new production in the subarctic Pacific, J. Geophys. Res., 96, 741-748, 1991.

Baum, R., Adding iron to ocean makes waves as way to cut greenhouse CO_2, Sci. Technol., July 2, 1990.

Broecker, W. S., T.-H. Peng, G. Ostlund, and M. Stuiver, The distribution of bomb radiocarbon in the ocean, J. Geophys. Res., 90, 6953-6970, 1985.

De Baar, H. J., A. G. J. Buma, R. F. Nolting, G. C. Cadee, G. Jacques, and P. J. Treguer, On iron limitation of the southern ocean: Experimental observations in the Weddell and Scotia Seas, Mar. Ecol. Prog. Ser., 65, 105-122, 1990.

Dugdale, R. C., and F. P. Wilkerson, Iron addition experiment in the Antarctic: A reanalysis, Global Biogeochem. Cycles, 4, 13-19, 1990.

Eppley, R. W., and B. J. Peterson, Particulate organic matter flux and planktonic new production in the deep ocean, Nature, 282, 677-680, 1979.

Friedli, H., H. Loetscher, H. Oeschger, U. Siegenthaler, and B. Stauffer, Ice core record of the $^{13}C/^{12}C$ ratio of atmospheric carbon dioxide in the past two centuries, Nature, 324, 237-238, 1986.

Intergovernmental Panel on Climate Change (IPCC), Scientific Assessment of Climate Change, United Nations Environment Programme/World Meteorological Organization, Geneva, 1990.

Joos, F., J. L. Sarmiento, and U. Siegenthaler,
   Estimates of the effect of southern ocean iron
   fertilization on atmospheric CO_2 concentrations,
   Nature, 349, 772-775, 1991.
Keeling, C. D., R. B. Bacastow, A. F. Carter, S. C.
   Piper, T. P. Whorf, M. Heimann, W. G. Mook,
   and H. Roeloffzen, A three-dimensional model of
   atmospheric CO_2 transport based on observed
   winds, 1, Analysis of observational data, in Aspects
   of Climate Variability in the Pacific and the Western
   Americas, Geophys. Monogr. Ser., vol 55, edited
   by D. H. Peterson, pp. 165-236, AGU,
   Washington, D.C., 1989.
Knox, F., and M. B. McElroy, Changes in
   atmospheric CO_2: Influence of the marine biota at
   high latitudes, J. Geophys. Res., 89, 4624-4637,
   1984.
Legendre, L., and M. Gosselin, New production and
   export of organic matter to the deep ocean:
   Consequences of some recent discoveries, Limnol.
   Oceanogr., 34, 1374-1380, 1989.
Levitus, S., Climatological atlas of the world ocean,
   133 pp., NOAA Prof. Pap. 13, U.S. Gov. Printing
   Off., Washington, D. C., 1982.
Martin, J. H., Glacial-interglacial CO_2 change: The
   iron hypothesis, Paleoceanography, 5, 1-13, 1990.
Martin, J. H., and S. E. Fitzwater, Iron deficiency
   limits phytoplankton growth in the north-east
   Pacific subarctic, Nature, 331, 341-343, 1988.
Martin, J. H., and R. M. Gordon, Northeast Pacific
   iron distributions in relation to phytoplankton
   productivity, Deep Sea Res., 35, 177-196, 1988.
Martin, J. H., R. M. Gordon, S. E. Fitzwater, and
   W. W. Broenkow, VERTEX: Phytoplankton/iron
   studies in the Gulf of Alaska, Deep Sea Res., 36,
   649-680, 1989.
Martin, J. H., S. E. Fitzwater, and R. M. Gordon,
   Iron deficiency limits phytoplankton growth in
   Antarctic waters, Global Biogeochem. Cycles, 4, 5-
   12, 1990a.
Martin, J. H., R. M. Gordon, and S. E. Fitzwater,
   Iron in Antarctic waters, Nature, 345, 156-158,
   1990b.
Najjar, R. G., Simulations of the phosphorus and
   oxygen cycles in the world ocean using a general
   circulation model, p. 127, Ph.D. thesis, Princeton
   Univ., Princeton, N.J., 1990.
Neftel, A., E. Moor, H. Oeschger, and B. Stauffer,
   Evidence from polar ice cores for the increase in
   atmospheric CO_2 in the past two centuries, Nature,
   315, 45-47, 1985.
Peng, T.-H., and W. S. Broecker, Dynamic
   limitations on the Antarctic iron fertilization
   strategy, Nature, 349, 227-229, 1991.
Peng, T.-H., T. Takahashi, and W. S. Broecker,
   Seasonal variability of carbon dioxide, nutrients and
   oxygen in the North Atlantic surface water:
   Observations and a model, Tellus, Ser. B, 39, 439-
   458, 1987.
Sarmiento, J. L., and J. R. Toggweiler, A new model

for the role of the oceans in determining
   atmospheric P_{CO_2}, Nature, 308, 621-624, 1984.
Sarmiento, J. L., T. D. Herbert, and J. R.
   Toggweiler, Causes of anoxia in the world ocean,
   Global Biogeochem. Cycles, 2, 115-128, 1988.
Siegenthaler, U., and H. Oeschger, Biospheric CO_2
   emisssion during the past 200 years reconstructed
   by deconvolution of ice core data, Tellus, Ser. B,
   39, 140-154, 1987.
Siegenthaler, U., and T. Wenk, Rapid atmospheric
   CO_2 variations and ocean circulation, Nature, 308,
   624-625, 1984.
Siegenthaler, U., H. Friedli, H. Loetscher, E. Moor,
   A. Neftel, H. Oeschger, and B. Stauffer, Stable-
   isotope ratios and concentration of CO_2 in air from
   polar ice cores, Ann. Glaciol., 10, 1-6, 1988.
Takahashi, T., W. S. Broecker, and A. E.
   Bainbridge, Supplement to the alkalinity and total
   carbon dioxide concentration in the world oceans, in
   Carbon Cycle Modelling, SCOPE 16, edited by B.
   Bolin, pp. 159-199, John Wiley, New York, 1981.
Takahashi, T., W. S. Broecker, and S. Langer,
   Redfield ratio based on chemical data from
   isopycnal surfaces, J. Geophys. Res., 90, 6907-
   6924, 1985.
Toggweiler, J. R., Is the downward DOM flux
   important in carbon transport?, in Productivity of
   the Ocean: Present and Past, edited by W. H.
   Berger et al., pp. 65-83, John Wiley, New
   York,1989.
Warner, M. J., Chlorofluoromethanes F-11 and F-12:
   Their solubilities in water and seawater and studies
   of their distributions in the South Atlantic and North
   Pacific Oceans, Ph.D. thesis, Univ. of Calif., San
   Diego, 1988.
Warner, M. J., and R. F. Weiss, Solubilities of
   chlorofluorocarbons 11 and 12 in water and
   seawater, Deep Sea Res., 17, 721-735, 1985.
Weiss, R. F., J. L. Bullister, M. J. Warner, F. A.
   Van Woy, and P. K. Salameh, AJAX Expedition
   chlorofluorocarbon measurements, Ref. 90-6,
   Scripps Inst. of Oceanogr., La Jolla, Calif., 1990.
Wenk, T., and U. Siegenthaler, The high-latitude
   ocean as a control of atmospheric CO_2, in The
   Carbon Cycle and Atmospheric CO_2: Natural
   Variations Archean to Present, Geophys. Monogr.
   Ser., vol. 32, edited by E. T. Sundquist and W. S.
   Broecker, pp. 185-194, AGU, Washington, D. C.,
   1985.

   F. Joos and U. Siegenthaler, Physics Institute,
University of Bern, CH-3012 Bern, Switzerland.
   J. L. Sarmiento, Atmospheric and Ocean Sciences
Program, Princeton University, Princeton, NJ 08544.